

Statistical Analysis and Modeling of the Geometry and Topology of Plant Roots

Guan Wang, Hamid Laga, Jinyuan Jia, Stanley J. Miklavcic, Anuj Srivastava

Abstract—Root is an important organ of a plant since it is responsible for water and nutrient uptake. Analyzing and modelling variabilities in the geometry and topology of roots can help in assessing the plant's health, understanding its growth patterns, and modeling relations between plant species and between plants and their environment. In this article, we develop a framework for the statistical analysis and modeling of the geometry and topology of plant roots. We represent root structures as points in a tree-shape space equipped with a metric that quantifies geometric and topological differences between pairs of roots. We then use these building blocks to compute geodesics, *i.e.*, optimal deformations under the metric, between root structures, and to perform statistical analysis of a population of roots. We demonstrate the utility of the proposed framework on a dataset of wheat roots grown in different environmental conditions. We will also show that the framework can be used in various applications including classification and symmetry analysis.

Keywords: geodesics, tree-shape space, root shape alignment, shape analysis, principal component analysis, shape modeling, root shape synthesis

1 INTRODUCTION

Roots are the primary site of nutrient and water uptake for plants and play a crucial role in plant growth. Understanding structural (*i.e.*, geometric and topological) similarities and dissimilarities between roots, and capturing and modeling the structural variability in root populations can help in assessing the plant's health, understanding its interaction with the surrounding environment, and modelling growth processes.

Existing techniques for modelling structural variability are limited to objects that only bend and stretch [1], [2], [3], [4]. Early works, *e.g.*, [1], use morphable models, which represent the shape of an object using a dense set of landmarks and thus it can be seen as a point in a high-dimensional Euclidean space. Statistical analysis can then be performed using standard techniques such as principal component analysis. However, these techniques are limited to objects which only slightly bend or stretch. Recent works such as [2], [3], [4] proposed new formulations that are suitable for large elastic deformations. These techniques, however, do not handle topological variations such as those encountered in natural objects that have a tree structure, *e.g.*, plant's shoots or roots, airway trees, and neuronal structures

in the human brain. In these types of objects, growth processes, disease progression, and environmental effects affect not only their geometry but also their branching structures.

In this paper, we propose a framework for the statistical analysis of the shape and structure of objects that have a tree structure. We focus on plant roots characterised by a main root and lateral roots of single order; higher order laterals (sub laterals and off laterals) are not catered for in the present form, although the model can be extended to treat these as well. In the meantime, we foresee that actual and more complex root systems are dissected to attain the form applicable to the analysis presented in this paper.

The framework presented in this paper builds on the representation proposed by Duncan *et al.* [5] for the analysis of simple neuronal structures. It allows to:

- Compute correspondences and geodesic paths between plant roots even when undergoing large bending, stretching, and topological deformations.
- Compute statistical atlases, *i.e.*, means and principal modes of variation, of plant root collections.
- Characterize the geometric and structural variability within a collection of roots using probability distributions.
- Develop a mechanism for synthesizing plant roots either randomly, using random sampling, or in a controlled manner using regression from biologically motivated parameters.

The proposed framework has a wide range of applications. We show its utility in symmetry analysis and in root classification. It also has multiple applications in plant biology. It can be applied to quantify differences in root morphology. It can also be used to compare root systems of either different genotypes grown under the same environmental conditions, or root systems of the same genotype plant grown under different environmental conditions, including different nutrient concentrations, or soils at different levels of moisture content, or soils of different toxicity.

- Guan Wang and Jinyuan Jia are with School of Software Engineering, Tongji University, China. E-mail: guan.wang@tongji.edu.cn
- Hamid Laga is with the Information Technology, Mathematics and Statistics Discipline, Murdoch University (Australia), and with the Phenomics and Bioinformatics Research Centre, University of South Australia. E-mail: H.Laga@murdoch.edu.au
- Stanley J. Miklavcic is with the Phenomics and Bioinformatics Research Centre, University of South Australia.
- Anuj Srivastava is with Department of Statistics, Florida State University, USA.

The remaining parts of this paper are organised as follows; Section 2 overviews the related work. Section 3 lays down the mathematical formulation of the concept of tree-shape space and its associated metric. The proposed concepts of tree-shape space, metrics, and geodesics are then used to perform statistical analysis of collections of plant roots (Section 4), and to synthesize and simulate 3D plant roots (Section 5). Section 6 presents the results, and compares the performance of the proposed approach and the quality of its results with the state-of-the-art. Section 7 summarizes the main finding of this paper.

2 RELATED WORKS

The framework developed in this article can be seen as the generalization to objects with tree-like structures, *e.g.*, plant roots and shoots of the statistical analysis techniques that have been proposed for manifold 3D shapes. These types of objects vary not only in geometry but also in topology. Thus, we focus our survey on the techniques which have been proposed for capturing root morphology, and on techniques for statistical shape analysis.

2.1 Root morphology analysis

Quantitative characterization of root shapes can reveal fine differences between various phenotypes, signals, and exogenous regulatory substances [6]. This can facilitate molecular-genetic and physiological studies of root development. Some approaches extract shape descriptors to capture the important geometric and morphological properties of root shapes. Examples of such properties include the angular deviation of root tip from vertical axis [7], [8], [9], the vertical growth index [6], [10], which is measured as the ratio between the root tip ordinate and the root length, and the horizontal growth index defined as the ratio between the root tip abscissa and the root length. Schultz *et al.* [11], on the other hand, employed straightness, wave density, and horizontal growth index to describe the root shape.

These shape descriptors have been used to represent and compare root shapes in the descriptor space. They, however, only represent spatial information about roots. Also, variability in the descriptor space often does not correspond to variability in root shapes. For example, the average of two root descriptors is not guaranteed to correspond to the average root, not even to a valid root shape.

2.2 Statistical Shape analysis and modeling

Instead of using descriptors to characterize the shape of objects, several recent papers treat the shape of an object as a point in a shape space. Equipping the shape space with a proper metric allows comparing objects based on their shapes, computing geodesics, and performing statistical analysis including regressions and shape synthesis. These concepts have been extensively investigated in the case of 3D manifold objects such as human faces [1], human bodies [12], arbitrary natural objects [2], [3], and man-made objects [13]. These methods, however, are limited to 3D models with fixed topology. They cannot capture and model structural variabilities such as those present in plant roots.

More closely related to our approach are techniques based on tree statistics. The seminal work of Billera *et al.* [14] proposed the notion of continuous tree-space and its associated tools for computing summary statistics. Some variants of this idea have been introduced for statistical analysis of tree-structured data, *e.g.*, [15], [16]. These works, however, only consider the topological structure of trees and ignore the geometric attributes of edges, which limits their usage. To overcome this limitation, several extended methods have been proposed for defining a more general tree-space. This includes Feragen *et al.*'s framework [17], [18], [19], [20], which proposed a tree-shape space for computing statistics of airway trees, and its extension to complex botanical trees [21], [22].

Despite their efficiency and accuracy in certain situations, these techniques exhibit three main fundamental limitations. First, they use the Quotient Euclidean Distance (QED), which is not suitable for capturing large elastic deformation, *i.e.*, bending and stretching, of the branches. Second, they represent tree shapes as *father-child branching* structure, which leads to significant shrinkage along the geodesics between trees that exhibit large topological differences. Third, branch-wise correspondences need to be manually specified, especially when dealing with complex tree-like structures, which restricts its utility in practical applications.

In contrast, we propose a statistical framework, which is more suitable for analyzing plant root shapes. It builds upon and extends the recent work of Adam *et al.* [5], which showed that *main-side branching* representation is more efficient for capturing topological changes. To the best of our knowledge, this is the first approach that deals with statistical modeling of plant root shapes. We demonstrate through experiments that this framework can produce reasonable statistical summaries. It also enables root shape synthesis, either randomly or in a controlled manner, and root classification based on their shape.

3 MATHEMATICAL REPRESENTATION AND SHAPE SPACE METRIC

The input to our framework is a collection of 2D plant roots. We first skeletonize each root and convert it into a set of two-layer planar curves: $\beta = (\beta_0, \{\beta_i\}_{i=1}^n)$. Here, β_0 represents the main root branch and $\{\beta_i\}_{i=1}^n$ represent the finite (possibly empty) set of lateral branches, each one is attached to the main root at some locations, see Figure 1. Each branch β_i is a continuous curve in \mathbb{R}^2 , *i.e.*, $\beta_i : [0, 1] \rightarrow \mathbb{R}^2$. Let $t_i \in [0, 1]$ such that $\beta_0(t_i) = \beta_i(0)$ is the location on β_0 to which the i -th lateral branch β_i is attached.

In order to perform statistical analysis of the geometry and topology of a collection of such roots, we need to define a tree-shape space, a metric on this space, and a mechanism for computing correspondences and geodesics in the tree-shape space. Due to their arbitrary structure, two roots will rarely have the same number of lateral roots. To simplify the search for correspondences, and following [5], we augment each root β by adding virtual lateral branches, *i.e.*, branches of length zero, according to the t value of each non-virtual lateral branch. For example, for two roots $\beta_1 = (\beta_0^1, \{\beta_i^1\}_{i=1}^{n_1})$ and $\beta_2 = (\beta_0^2, \{\beta_i^2\}_{i=1}^{n_2})$, we add n_2

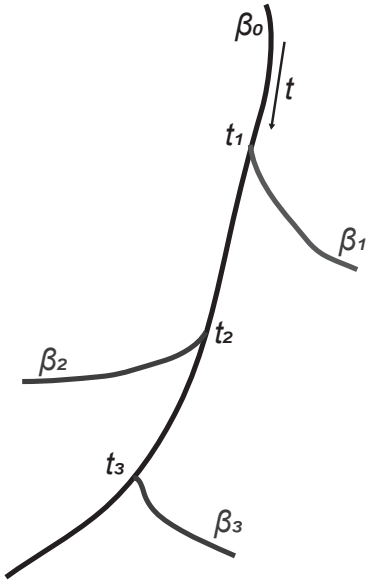


Fig. 1: The representation of a simple plant root.

null branches to β_1 , whose locations on β_0^1 are computed as $t_{n_1+i}^1 = t_i^2, i = 1, 2, \dots, n_2$. Then, we add n_1 null branches to β_2 in the same manner. In what follows, and for simplicity of notation, we will also use the symbol β to indicate an augmented root.

We represent each root β using its Square Root Velocity Function Tree (SRVFT) [23], \mathbf{q} , which consists of a collection of Square Root Velocity Functions, one for each branch β in β . That is, given one branch β , its SRVF representation is defined as its derivative scaled by the square-root of the \mathcal{L}_2 norm of the derivative:

$$q(t) = \begin{cases} \frac{\dot{\beta}(t)}{\sqrt{\|\dot{\beta}(t)\|}} & \text{if } \dot{\beta}(t) \text{ exists and is nonzero.} \\ 0 & \text{otherwise} \end{cases} \quad (1)$$

As such, the SRVF is translation invariant. Thus, when converting an entire root into its SRVFT representation, we lose track of the location of the bifurcation points. In order to preserve them, we represent each side branch using an ordered pair (q_i, s_i) where $s_i \in [0, 1]$ is the starting location on β_0 . Then, the SRVFT representation of the entire root β becomes $\mathbf{q} = (q_0, \{(q_i, s_i)\}_{i=1}^N)$.

Let \mathcal{C} denote the space of all root shapes, which are represented by their SRVFTs. \mathcal{C} is called *pre-shape space* [23]. We now need to define the metric and the mechanism for computing geodesics between a pair of roots.

3.1 Metric for tree-like shapes

Our goal is to define a metric, which quantifies the geometric, *i.e.*, bending and stretching, and topological deformations. We follow the approach of Duncan *et al.* [5]. Let $\mathbf{q}^i = (q_0^i, \{(q_k^i, s_k^i)\}_{k=1}^N)$, $i \in \{1, 2\}$ be the SRVFT representations of two roots β_1 and β_2 . We define the distance, or dissimilarity, between such roots in \mathcal{C} as:

$$d_{\mathcal{C}}(\mathbf{q}^1, \mathbf{q}^2) = \lambda_m \|q_0^1 - q_0^2\|^2 + \lambda_s \sum_{k=1}^N \|q_k^1 - q_k^2\|^2 + \lambda_p \sum_{k=1}^N (s_k^1 - s_k^2)^2, \quad (2)$$

which is a weighted sum of three terms. The first term is the \mathcal{L}_2 distance between the main roots. Since the \mathcal{L}_2 distance in the SRVF space is equivalent to the full elastic metric in the space of curves [23], then the first term measures the amount of bending and stretching needed to align one curve onto the other. The second term is the \mathcal{L}_2 distance between the SRVFs of the lateral roots. The last term measures the distance between the bifurcation points and is used to capture topological changes. The parameters $\lambda = (\lambda_m, \lambda_s, \lambda_p)$ control the relative contribution of the three terms.

A good metric for statistical shape analysis should be invariant to shape-preserving transformations, *i.e.*, translation, scaling, rotation, and re-parameterization. The SRVF representation is translation-invariant by construction since it uses the derivatives. Invariance to scale can be efficiently handled by scaling each root by the length of its main root. Note that the latter might not be needed depending on the application at hand. For instance, growth analysis requires preserving the scales of the roots.

The remaining variabilities, *i.e.*, rotation and reparameterization, are handled algebraically following [4], [5]. The action of all possible rotations $O \in SO(2)$ and reparameterizations $\gamma \in \Gamma$ on a root shape β forms a set of roots that have the same shape (Γ here is the space of all orientation-preserving diffeomorphisms of $[0, 1]$ to itself). Similar to [4], we redefine the dissimilarity between two roots β_1 and β_2 as the length of the shortest geodesic between \mathbf{q}^1 and $O(\mathbf{q}^2, \gamma)$ (here, (\mathbf{q}, γ) is the SRVFT of $\beta \circ \gamma$):

$$d(\beta_1, \beta_2) = \min_{O \in SO(2), \gamma \in \Gamma} d_{\mathcal{C}}(\mathbf{q}^1, O(\mathbf{q}^2, \gamma)), \quad (3)$$

where $d_{\mathcal{C}}(\mathbf{q}^1, O(\mathbf{q}^2, \gamma))$ is the length of the geodesic between \mathbf{q}^1 and the rotated and re-parameterized version of \mathbf{q}^2 . The optimization over O and γ is the registration process, which consists of searching for optimal alignment and correspondence between β_1 and β_2 . It is solved as a linear assignment problem following [5].

3.2 Geodesics

A geodesic is the optimal deformation (bending, stretching, and topological changes), under the metric, from one root to another. Its length quantifies the minimum amount of deformation that one needs to apply to one root in order to align it onto the other. For simplicity, let us also denote by \mathbf{q}^2 the version of \mathbf{q}^2 after applying the optimal rotation and reparameterization found by optimizing Equation (3). Since the distance between \mathbf{q}^1 and \mathbf{q}^2 is a weighted sum of Euclidean distances, see Equation (2), then the geodesic α connecting them is the linear path that connects the two points, *i.e.*, :

$$\alpha(r) = (1 - r)\mathbf{q}^1 + r\mathbf{q}^2, 0 \leq r \leq 1, \quad (4)$$

which is defined in the SVFT space. The geodesic between β_1 and β_2 is then given by mapping the path α back to the space of trees.

Figure 2 shows an example of a geodesic between two simple trees that differ in topology. For this example we also show the results obtained by the approach of Feragen *et al.* [19] and the approach of Wang *et al.* [21]. Each row in the figure is one geodesic between the leftmost and rightmost roots. Branchwise correspondences are indicated using

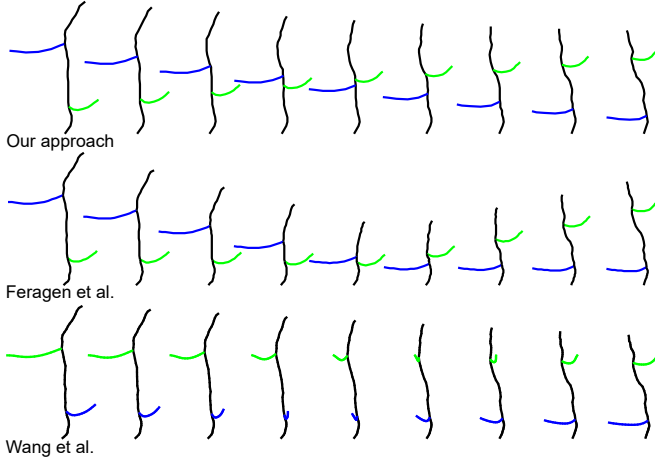


Fig. 2: Comparison between the geodesics obtained using our method (top row, $\lambda_m = 0.02$, $\lambda_s = 1.0$, $\lambda_p = 1.0$), the approach of Feragen *et al.* [19] (middle row), and the approach of Wang *et al.* [21] (bottom row). The colors indicate branchwise correspondences.

colors. In this example, we can see that the intermediate roots along the geodesic obtained using [19] are not natural; they exhibit unnatural shrinkage and are unable to find the correct correspondences. The approach of Wang *et al.* [21] is less prone to global shrinkage. However, as seen in the last row of Figure 2, it can match branches located in different sides. As such, the lateral branches unnaturally shrink and expand along the geodesic.

4 STATISTICAL ATLAS

For a given set of root samples, denoted as $\{\beta_i, i = 1, 2, \dots, m\}$, the mean root is defined as the root that is as close as possible to all the roots in the set. Mathematically, it is the root that minimizes the sum of the geodesic distances to all the roots. Similar to geodesic computation, we first add to every root β_i virtual lateral branches to equalize the number of lateral branches across the roots in the dataset. Let μ be the SRVFT representation of the mean root. It can be computed as:

$$\mu = \underset{q \in \mathcal{S}, O \in SO(2), \gamma \in \Gamma}{\operatorname{argmin}} d_C(q, O(q^i, \gamma)). \quad (5)$$

Here, \mathcal{S} is the tree-shape space. The solution to Equation (5) is known as the Karcher mean. We employ the same gradient descent approach described in [4] to solve this optimization problem.

Figure 3(a) shows the mean root of three roots generated by this approach. Figure 3(b) compares between the mean roots generated by our approach, the approach of Feragen *et al.* [19], and the approach of Wang *et al.* [21]. It can be clearly seen that the mean root generated by our approach is more plausible than those generated by the other two methods.

In addition to the mean root, which can be regarded as a template that characterizes the main morphological properties of the shape of roots in the dataset, one would also like to (1) quantify how the samples in the dataset deviate from the mean root, and (2) analyze the distribution

of roots around the mean root. This can be done by computing the covariance matrix and the modes of variation. The tree-shape space \mathcal{S} is a non-linear manifold, thus we employ its tangent space $T_\mu(\mathcal{S})$ instead of \mathcal{S} to perform statistical analysis. Similar to [23] [4], we first map each q^i onto the tangent space using the inverse exponential map: $q^i \rightarrow v^i = \log_\mu(q^i)$. Then we calculate the covariance matrix: $C = \frac{1}{m-1} \sum_{i=1}^m v^i (v^i)^t$. After calculating the eigenvalues and eigenvectors of C , we can obtain the principal modes of shape variation for the root collection. We can generate a sample $v_k \in T_\mu(\mathcal{S})$ along each eigenvector Λ_i as: $v_k = \alpha \sqrt{\lambda_i} \Lambda_i$, $\alpha \in \mathbb{R}$ on the tangent space, where λ_i is the eigenvalue associated with the eigenvector Λ_i .

5 PLANT ROOTS SYNTHESIS

5.1 Root synthesis by random sampling

The eigenvectors $\{\Lambda_i\}$ form an orthonormal basis of a Euclidean vector space. One can characterize the distribution of the input roots by fitting probability models either from a non-parametric family by computing their probability densities directly from the data, or from a parametric family, such as multivariate Gaussian. In this paper, for the sake of simplicity, we fit to the population a multivariate Gaussian with mean μ and a diagonal covariance matrix C whose diagonal elements are the square roots of the eigenvalues λ_i .

Once we have the probability model, a new botanical tree can be generated by randomly sampling from the distribution. In the case of a Gaussian model, a random root can be synthesized by first randomly generating m real values $b_1, b_2, \dots, b_n \in \mathbb{R}$ and setting

$$q = \operatorname{Exp}_\mu \left(\sum_{i=1}^m b_i \sqrt{\lambda_i} \Lambda_i \right). \quad (6)$$

Here, Exp_μ is the exponential map, which maps elements in the tangent space to \mathcal{S} at μ to the SRVFT space. A root x can be obtained by mapping q back to the tree-shape space. In this paper, we only consider the m -leading eigenvalues such that $\frac{\sum_{i=1}^m \lambda_i}{\sum_i \lambda_i} > 0.99$. In order to generate plausible roots, one can restrict b_i 's to be within a certain range, *e.g.*, $[-1, 1]$.

5.2 User-controlled roots synthesis

While random sampling from the multivariate Gaussian distribution provides an easy way of synthesizing new roots, it lacks control. In fact, sometimes, users would like to generate roots by just adjusting a few parameters, *e.g.*, biologically motivated parameters. In this paper, we formulate this problem as a regression in the tree-shape space. In particular, let $\mathbf{p} \in \mathbb{R}^l$ be the vector of l parameters. Let x be a point in the tree-shape space and q its SRVFT representation. From Equation (6), q can be represented as a real valued vector $\mathbf{b} = (b_1, b_2, \dots, b_m)^T$. If we assume that the relation between the biological parameters \mathbf{p} and the root to be linear, then the mapping can be represented using $m \times (l + 1)$ matrix \mathbf{M} such that:

$$\mathbf{M}[p_1, p_2, \dots, p_l, 1]^T = \mathbf{b}. \quad (7)$$

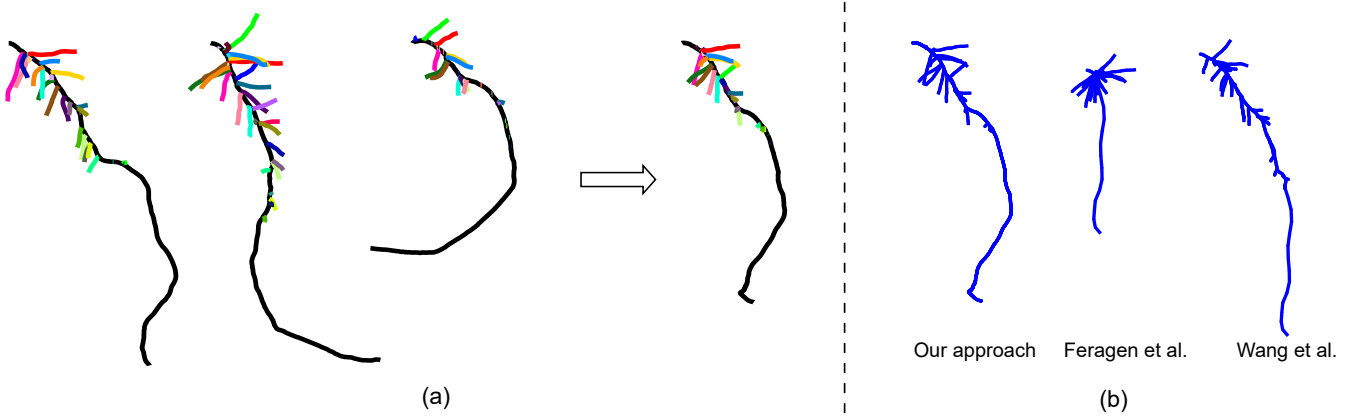


Fig. 3: (a) Mean root of three plant roots. Colors indicate branchwise correspondences. (b) Comparison with Feragen *et al.* [19] and Wang *et al.* [21].

After assembling all the parameter vectors into an $(l+1) \times m$ matrix \mathbf{P} and all the vectors \mathbf{b} into an $n \times m$ matrix \mathbf{B} , the mapping matrix \mathbf{M} can be calculated as follows;

$$\mathbf{M} = \mathbf{B}\mathbf{P}^+, \quad (8)$$

where \mathbf{P}^+ is the pseudoinverse of \mathbf{P} .

There are several biologically-motivated parameters that can be used. In this paper, we consider *the main root length*, *the mean length of the side-roots*, and *the standard deviation of the side root lengths*. We first extract these three parameters from a training dataset and use them to learn the regression model. At runtime, the user can specify these parameters and the system automatically synthesizes new root models.

6 RESULTS AND DISCUSSION

In this section, we consider a collection of wheat roots that exhibit different degrees of geometric and structural variations, and demonstrate the results of the proposed approach in computing (1) geodesics and (2) statistical summaries such as means and modes of variations. We also report the timing and compare our results to the state-of-the-art. Additional results are included in the supplementary material. For this, we have collected 53 wheat plant roots with rich structural variations. They were automatically skeletonized and converted into a two-layer structure representation as described in Section 3.

6.1 Geodesic and comparison

In this experiment, we consider pairs of plant roots, each pair is composed of a source and a target root, and generate new roots by computing the geodesic (optimal deformation) that connects the source to the target. Figure 4 shows two examples of such geodesics. For comparison, we also show geodesics between the same pair of roots but computed using the approaches of Feragen *et al.* [19] and of Wang *et al.* [21]. In each example, the colors indicate the branch-wise correspondences.

As one can see, the geodesics generated with the approach of Feragen *et al.* [19] exhibit unnatural shrinkage: the intermediate roots along the geodesic shrink and then expand. Also, the approach of Wang *et al.* [21] fails to

find correct branch-wise correspondences, which affects significantly the quality of the geodesics obtained with this approach. In comparison, the approach used in this paper is able to produce smooth geodesics with plausible-looking intermediate roots. More results are included in the supplementary material.

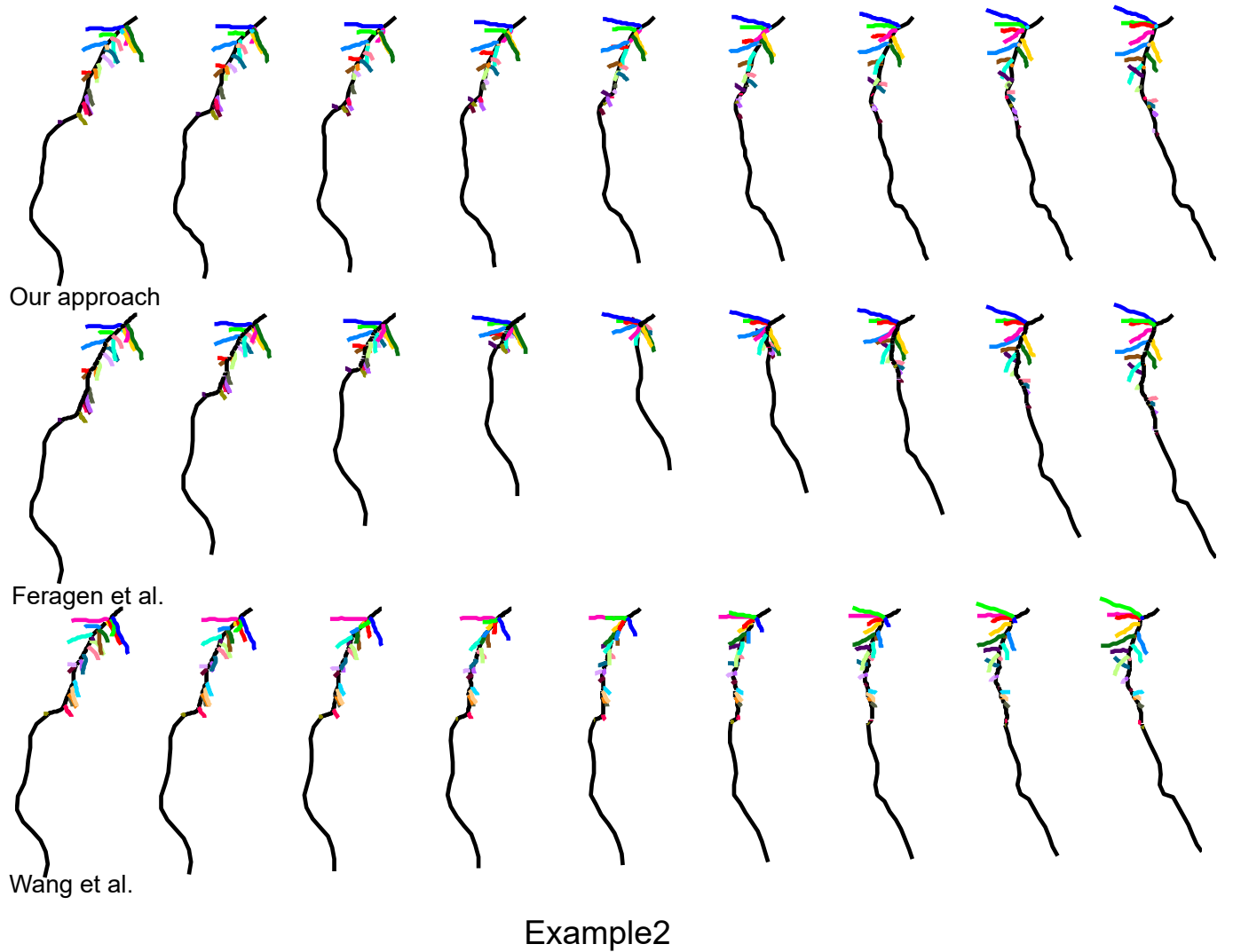
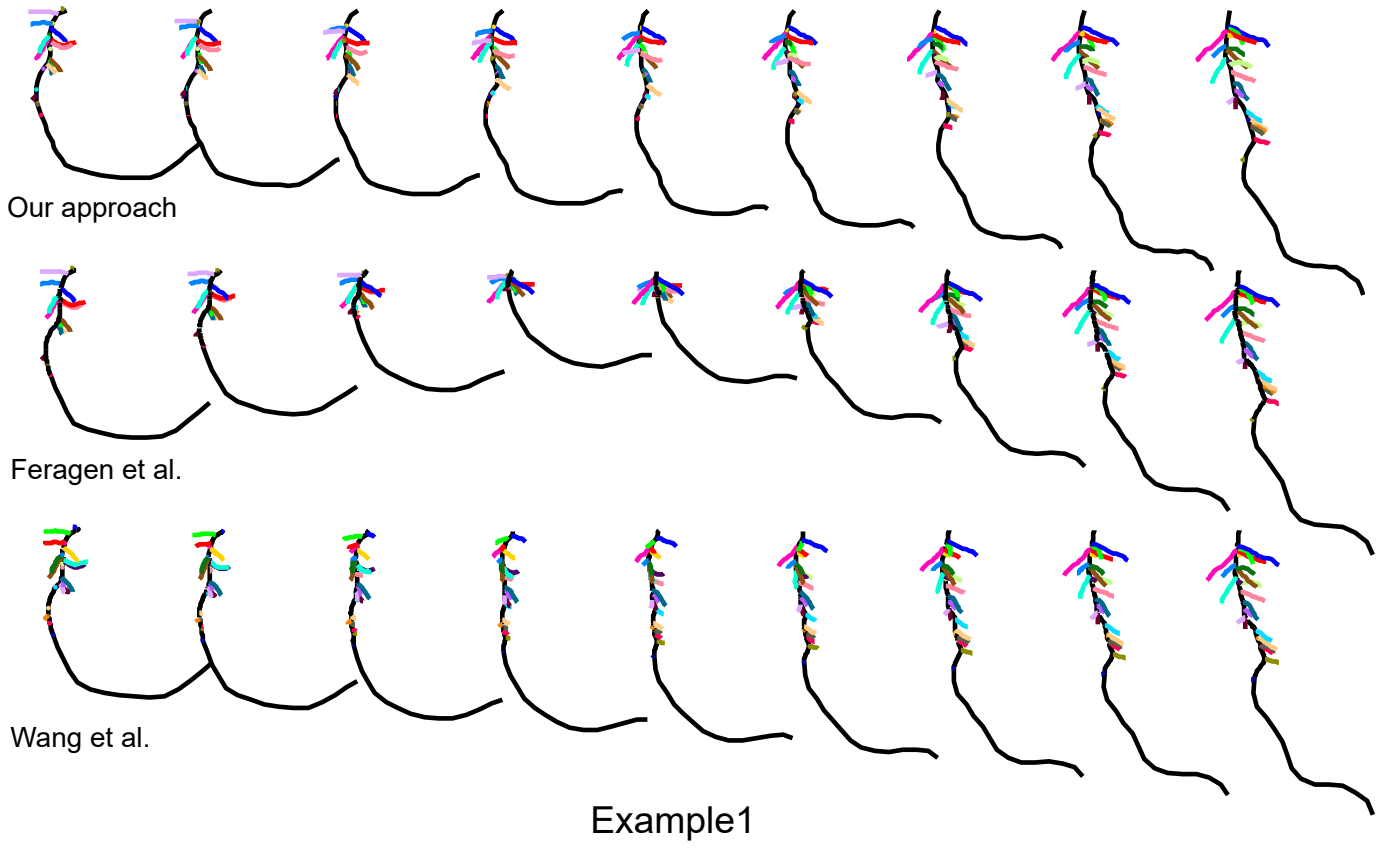
In addition, we check the influence of the weight λ_m, λ_s , and λ_p of Equation (2) on the quality of the geodesics. For the purpose of this experiment, we vary the values of these parameters and observe the results. This is illustrated in Figure 5 on a toy example. In the first three results where the triplet $(\lambda_m, \lambda_s, \lambda_p)$ is set to $(1.0, 0.01, 0.01)$, $(0.01, 1.0, 0.01)$, $(0.01, 0.01, 1.0)$, respectively, the three geodesics look very similar. However, in the fourth result where $\lambda_m = 0.01$, $\lambda_s = 0.00001$, and $\lambda_p = 1.0$, the approach favours the creation of new lateral branches rather than sliding the existing one. This is predictable since the last term, which measures distance between bifurcation points, is highly penalized.

The supplementary material also includes additional complex examples that show the effect of varying the parameters of Equation (2) on the quality of the geodesics.

6.2 Summary statistics

Figure 6 shows the mean root computed from the entire data set. The 53 input roots are shown on the left while the generated mean root is shown on the right. Note that the correspondences between each pair in the dataset, as well as between each sample in the dataset and the computed mean root, are automatically computed and do not require any user input or interaction. Also, the average of a pair of plant roots is a by-product of the geodesic computation process. In fact, the root that is equidistant to the source and the target roots is exactly their mean. Thus, the root that lies exactly at the middle of each geodesic in Figure 4 is actually the average of the leftmost and rightmost roots.

Figure 7 shows the first two principal modes of variation for the root dataset in Figure 6. From these results, we clearly see that the first two leading modes capture the main geometric and structural variation in the root dataset.



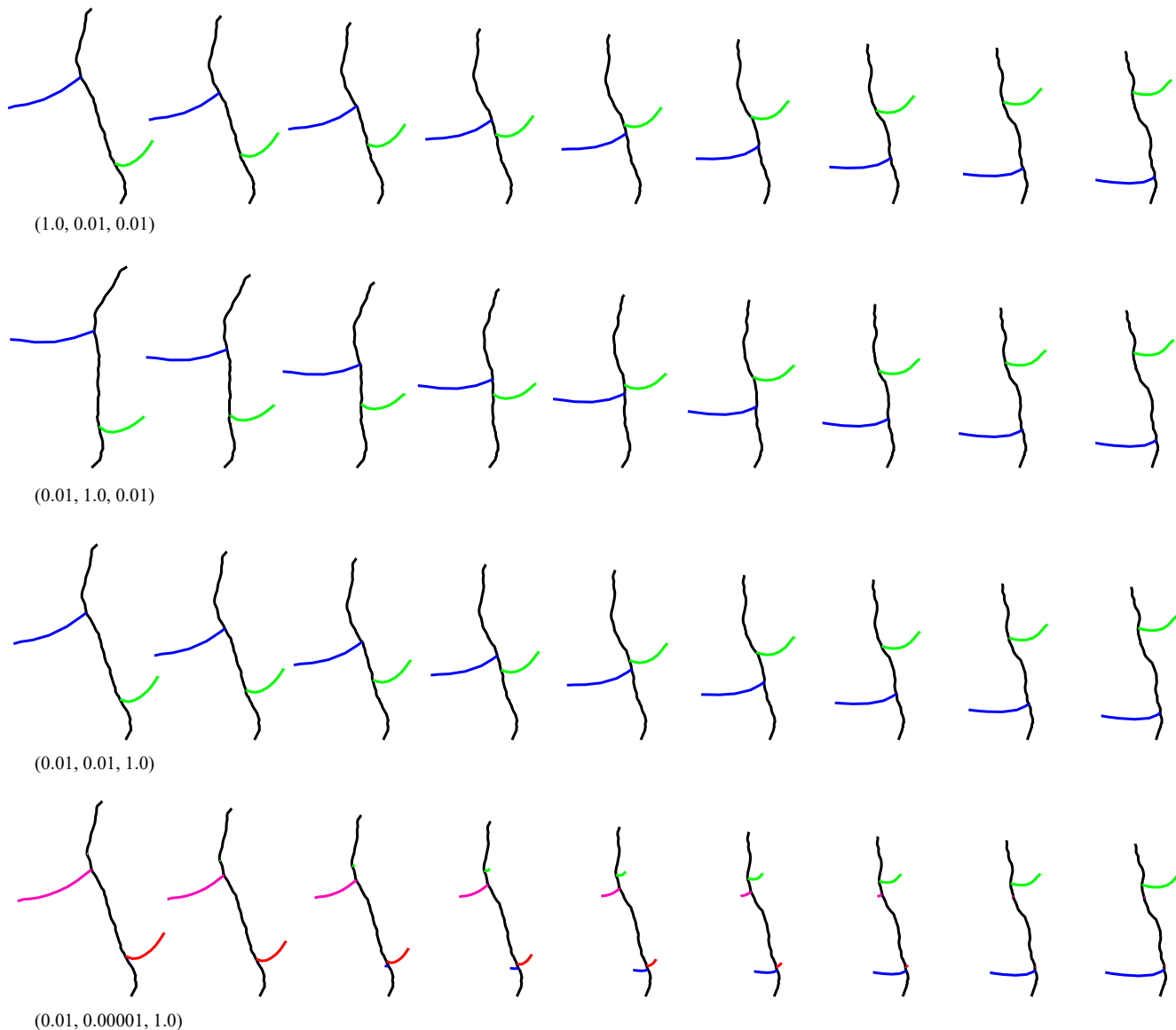


Fig. 5: The influence of parameters in Equation 2 on geodesic results of Figure 2 (by our approach). In the first three geodesics, we set $\lambda_m, \lambda_s, \lambda_p$ to be 1.0 and other two ones to be 0.01 respectively. In the fourth geodesic, we consider a more extreme case by setting $\lambda_m = 0.01, \lambda_s = 0.00001, \lambda_p = 1.0$. Colors indicate branch-wise correspondences.

6.3 Random root synthesis

Figure 8 shows plant roots that have been automatically synthesized by random sampling from the statistical model fitted to the root dataset of Figure 6. These roots have been synthesized without any biological knowledge or interaction from the users. For a better visualization, we group these synthesized plant roots into three clusters depending on their distances to the mean root. Note that the synthesized roots that are close to the mean share some similarities with the input roots but are not the same. The further the synthesized root deviates from the mean the less plausible it becomes.

6.4 User-controlled root synthesis

We show a few examples of plant roots generated with intuitive controls such as *main root length*, *mean length of side-roots*, and *standard deviation of side roots length*. We take the

plant roots of Figure 6, compute their mean root and their modes of variation, and then learn a regression model that maps the three control parameters into points in the tree-shape space. This provides a direct way to explore the range of root shapes. Figure 9, 10, 11 show a few representative results produced with this approach.

6.5 Timing

This framework has been implemented in Matlab and runs on a desktop PC with Intel(R) Core(TM) i5-4460 CPU@3.20GHz and 8GB of RAM. Table 1 reports the computation time for each geodesic shown in Figure 4. It also reports the side root number of the roots after adding virtual side roots.

To compute each of the geodesics of Figure 4, we first align the source and target roots to one another (alignment step), and then compute their geodesic using the method

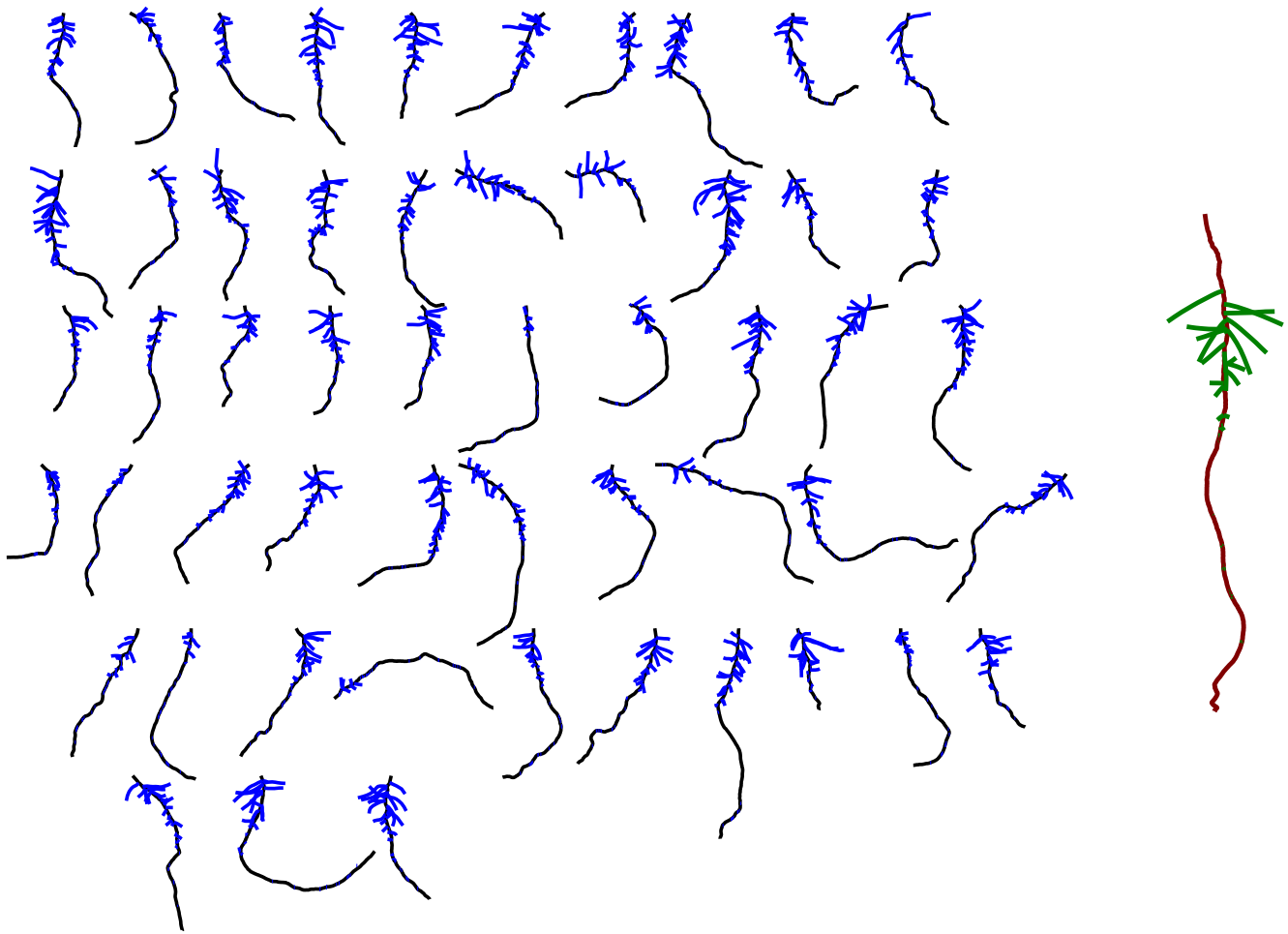


Fig. 6: Example of a mean root computed using the proposed approach. The input collection of 53 roots is shown on the left and the computed mean root is shown on the right with different colors. The mean root has been enlarged for visual clarity.

proposed in this paper, the method of Feragen *et al.* [19], and the method of Wang *et al.* [21]). Table 1 shows that most of the time has been consumed in the alignment process. Once roots are aligned, the method proposed in this article for computing geodesics is significantly faster than the approaches of Feragen *et al.* and Wang *et al.* (40 ms for ours vs. 11 s for the other two methods).

The computation of the mean root takes 9 hours 4 minutes. Once the mean root has been computed, computing the principal modes of variation takes 1.1 seconds. It only takes 0.22 seconds to generate one random root. For regression, it only takes 0.01 seconds to compute the mapping matrix M and about 0.001 seconds (on average) to generate a new root. This suggests that the approach proposed in this article is well suited for the generation and synthesis of root structures

6.6 Application to plant root classification

Finally, the length of the geodesic between two roots is a measure of dissimilarity between these roots. To demonstrate the utility of this measure for plant root classification, we computed the pairwise geodesic distance matrix for the

entire dataset and performed a hierarchical binary clustering using MATLAB's linkage function. Figure 13 shows the root clustering result according to the hierarchical binary clustering result as is shown in Figure 12. As one can see, the metric clusters together roots that have similar geometry and topology.

7 CONCLUSION AND FUTURE WORK

In this paper, we have developed a full framework for the statistical analysis and modeling of the geometry and topology of plant roots. Central to the framework is an elastic curve-based tree-shape space and an elastic metric that enables us to find optimal correspondences between roots, even in the presence of large topological deformations. As shown in the experimental results, the metric is suitable for comparing roots based on their shape, and for computing geodesics between them. We showed that the representation and metric can be used to compute statistical summaries of root collections and synthesize new roots either randomly or interactively by varying biologically-motivated parameters. This greatly simplifies the process of creating 2D root shapes. To the best of our knowledge, this

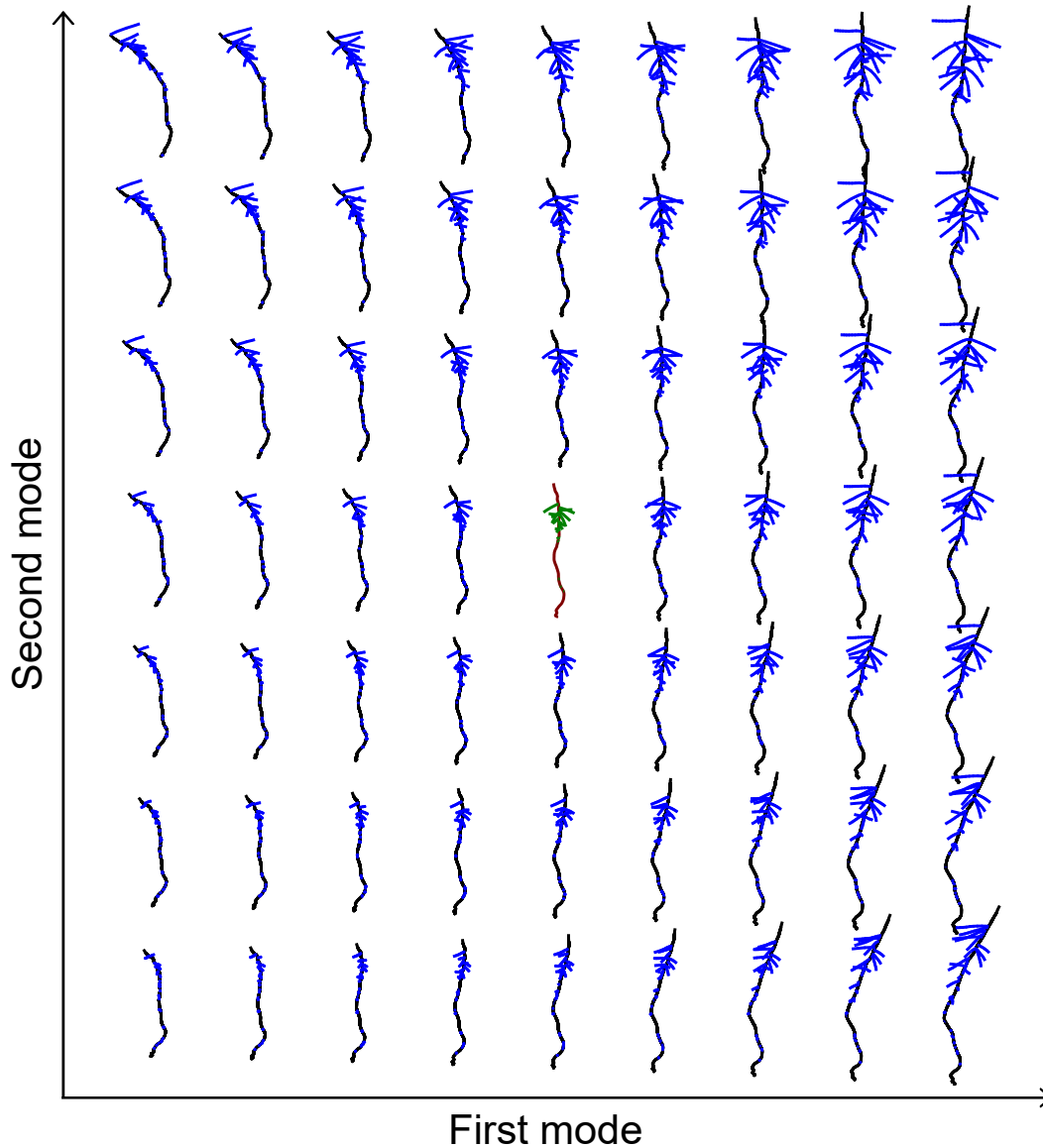


Fig. 7: The first two modes of variations computed on the dataset of Figure 6. The mean root in the centre of the array is highlighted using the same colors as of Figure 6.

is the first approach that dealt with the statistical modeling of the shape of roots.

Although effective as evidenced by the results shown in this paper, there are still some limitations that can be addressed in future work. First, we only considered roots that have two layers of branches. However, roots have complex tree structures often composed of more than two layers. In the future, we plan to extend the current framework to processing multi-layer roots. Second, the type of geodesic that our framework generates between a pair of trees depends on the weights of the three terms of the metric defined in Equation (2). While in this paper, we manually set these weights, it would be interesting to learn these parameters from data. Third, the regression framework proposed in this paper is data-driven and it just incorporates a few biological knowledge into the modeling process. Also, it does not take into account the environment effects, such as soil humidity, and nutrient content. In the future, it will be interesting

to incorporate these factors into the regression process and explore more regression tools beyond the linear ones.

Finally, we plan in the future to use the proposed framework in comparing root systems of either different genotypes grown under the same environmental conditions, or root systems of the same genotype plant grown under different environmental conditions, including different nutrient concentrations, or soils at different levels of moisture content, or soils of different toxicity. It can be also applied to quantify differences in root morphology. This could be achieved either by calculating the geodesic distance between mean roots (the average main roots plus laterals based on sets of roots taken/dissected from complete root systems of replicates of plants of one state) compared with geodesic distances determined within a set. Or, alternatively by computing the means of pairwise distances between roots of the two sets being compared.

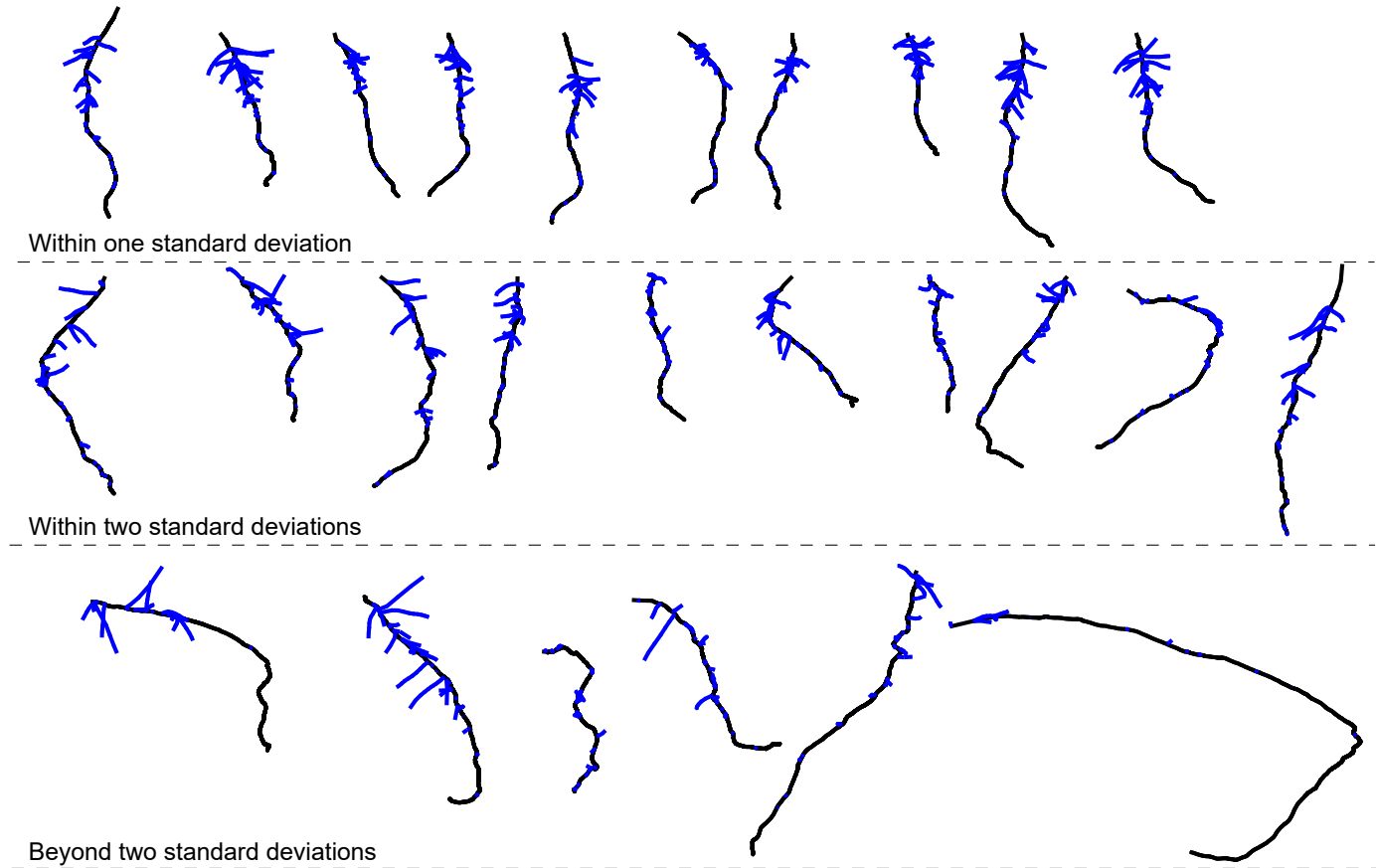


Fig. 8: Root shapes randomly sampled from the Gaussian distribution fitted to the root dataset of Figure 6.

TABLE 1: Comparison of the computation time (in seconds) between the proposed approach and the approaches of Feragen *et al.* [19] and Wang *et al.* [21]. "Size" refers to the number of lateral roots.

	Size	Approach	Alignment	Correspondence	Geodesic	Overall
Fig. 4 - Example 1	23	This paper	147.0	N/A	0.04	147.04
	23	Feragen <i>et al.</i> [19]	147.0	N/A	10.98	157.98
	23	Wang <i>et al.</i> [21]	147.0	0.0050	11.40	158.40
Fig. 4 - Example 2	14	This paper	137.0	N/A	0.04	137.04
	14	Feragen <i>et al.</i> [19]	137.0	N/A	10.60	147.60
	14	Wang <i>et al.</i> [21]	137.0	0.0028	11.31	148.31

Acknowledgement. The authors would like to thank Adam for sharing the code for analyzing simple neuronal trees, and Aasa Feragen for making the code for tree-like shape analysis publicly available. Guan Wang would like to thank the China Scholarship Council for funding his visit and stay at Murdoch University.

REFERENCES

- [1] V. Blanz and T. Vetter, "A morphable model for the synthesis of 3D faces," in *Proceedings of the 26th annual conference on Computer graphics and interactive techniques*. ACM Press/Addison-Wesley Publishing Co., 1999, pp. 187–194.
- [2] S. Kurtek, A. Srivastava, E. Klassen, and H. Laga, "Landmark-guided elastic shape analysis of spherically-parameterized surfaces," in *Computer Graphics Forum*, vol. 32, no. 2pt4. Wiley Online Library, 2013, pp. 429–438.
- [3] H. Laga, Q. Xie, I. H. Jermyn, A. Srivastava *et al.*, "Numerical inversion of snrf maps for elastic shape analysis of genus-zero surfaces," *IEEE Transactions on Pattern Analysis and Machine Intelligence*, vol. 39, no. 12, pp. 2451–2464, 2017.
- [4] H. Laga, S. Kurtek, A. Srivastava, and S. J. Miklavcic, "Landmark-free statistical analysis of the shape of plant leaves," *Journal of Theoretical Biology*, vol. 363, pp. 41–52, 2014.
- [5] A. Duncan, E. Klassen, and A. Srivastava, "Statistical shape analysis of simplified neuronal trees," *The Annals of Applied Statistics*, vol. 12, no. 3, pp. 1385–1421, 2018.
- [6] A. Grabov, M. Ashley, S. Rigas, P. Hatzopoulos, L. Dolan, and F. Vicente-Agullo, "Morphometric analysis of root shape," *New Phytologist*, vol. 165, no. 2, pp. 641–652, 2005.
- [7] A. Marchant, J. Kargul, S. T. May, P. Muller, A. Delbarre, C. Perrot-Rechenmann, and M. J. Bennett, "Aux1 regulates root gravitropism in *Arabidopsis* by facilitating auxin uptake within root apical tissues," *The EMBO Journal*, vol. 18, no. 8, pp. 2066–2073, 1999.
- [8] H. Fujita and K. Syōno, "Pis1, a negative regulator of the action of auxin transport inhibitors in *Arabidopsis thaliana*," *The Plant Journal*, vol. 12, no. 3, pp. 583–595, 1997.

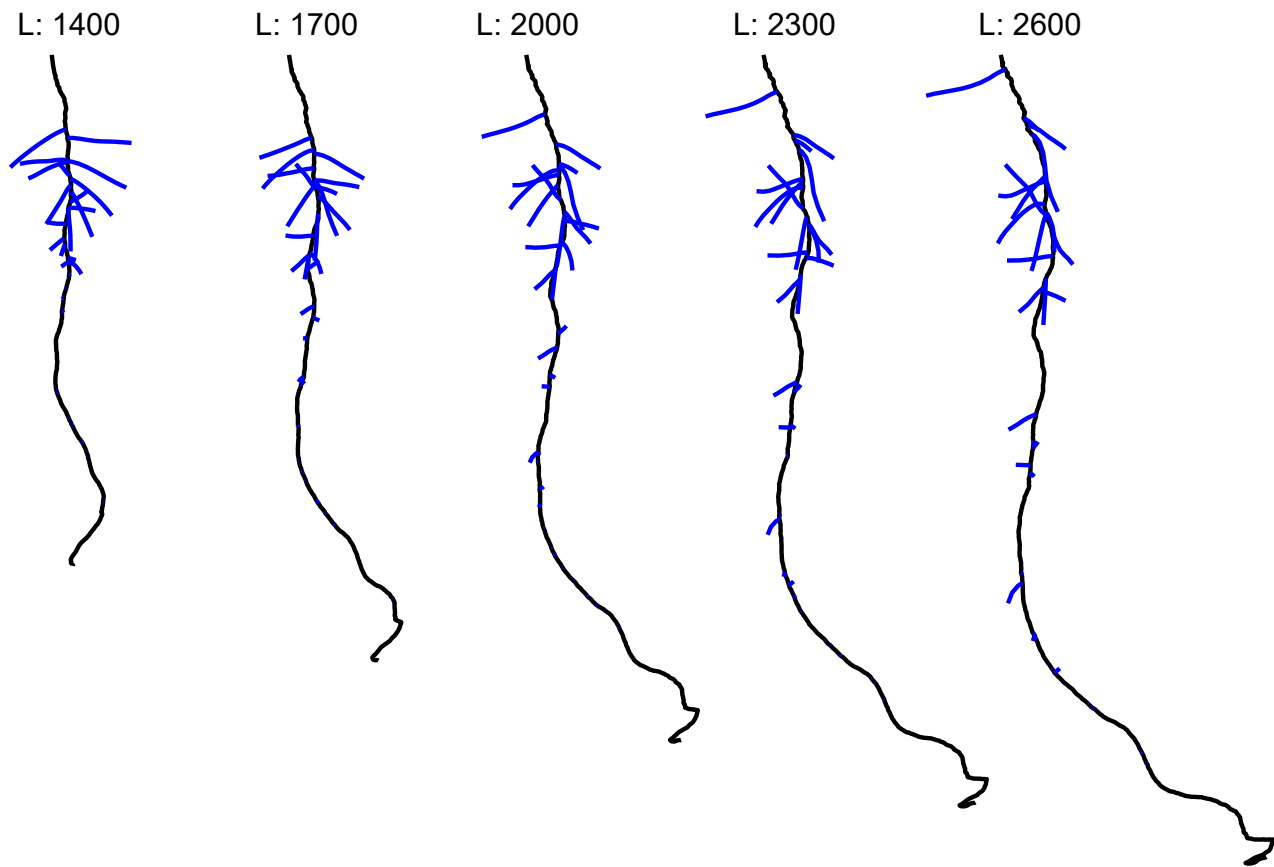


Fig. 9: Root shapes generated by user-specified control parameters. In this example, the user specifies the length of the main root, and the system automatically synthesizes root shapes.

- [9] H. Fujita and K. Syono, "Genetic analysis of the effects of polar auxin transport inhibitors on root growth in *Arabidopsis thaliana*," *Plant and Cell Physiology*, vol. 37, no. 8, pp. 1094–1101, 1996.
- [10] L. M. Vaughn and P. H. Masson, "A qtl study for regions contributing to *Arabidopsis thaliana* root skewing on tilted surfaces," *G3: Genes, Genomes, Genetics*, vol. 1, no. 2, pp. 105–115, 2011.
- [11] E. R. Schultz, A.-L. Paul, and R. J. Ferl, "Root growth patterns and morphometric change based on the growth media," *Microgravity Science and Technology*, vol. 28, no. 6, pp. 621–631, 2016.
- [12] B. Allen, B. Curless, and Z. Popović, "The space of human body shapes: reconstruction and parameterization from range scans," in *ACM Transactions on Graphics (TOG)*, vol. 22, no. 3. ACM, 2003, pp. 587–594.
- [13] H. Laga and H. Tabia, "Modeling and exploring co-variations in the geometry and configuration of man-made 3d shape families," in *Computer Graphics Forum*, vol. 36, no. 5. Wiley Online Library, 2017, pp. 13–25.
- [14] L. J. Billera, S. P. Holmes, and K. Vogtmann, "Geometry of the space of phylogenetic trees," *Advances in Applied Mathematics*, vol. 27, no. 4, pp. 733–767, 2001.
- [15] M. Owen and J. S. Provan, "A fast algorithm for computing geodesic distances in tree space," *IEEE/ACM Transactions on Computational Biology and Bioinformatics (TCBB)*, vol. 8, no. 1, pp. 2–13, 2011.
- [16] B. Aydın, G. Pataki, H. Wang, E. Bullitt, J. S. Marron *et al.*, "A principal component analysis for trees," *The Annals of Applied Statistics*, vol. 3, no. 4, pp. 1597–1615, 2009.
- [17] A. Feragen, F. Lauze, P. Lo, M. de Bruijne, and M. Nielsen, "Geometries on spaces of tree-like shapes," in *Asian Conference on Computer Vision*. Springer, 2010, pp. 160–173.
- [18] A. Feragen, S. Hauberg, M. Nielsen, and F. Lauze, "Means in spaces of tree-like shapes," in *Computer Vision (ICCV), 2011 IEEE International Conference on*. IEEE, 2011, pp. 736–746.
- [19] A. Feragen, P. Lo, M. de Bruijne, M. Nielsen, and F. Lauze, "Toward a theory of statistical tree-shape analysis," *IEEE Transactions on Pattern Analysis and Machine Intelligence*, vol. 35, no. 8, pp. 2008–2021, 2013.
- [20] A. Feragen, M. Owen, J. Petersen, M. M. Wille, L. H. Thomsen, A. Dirksen, and M. de Bruijne, "Tree-space statistics and approximations for large-scale analysis of anatomical trees," in *International Conference on Information Processing in Medical Imaging*. Springer, 2013, pp. 74–85.
- [21] G. Wang, H. Laga, N. Xie, J. Jia, and H. Tabia, "The shape space of 3D botanical tree models," *ACM Transactions on Graphics (TOG)*, vol. 37, no. 1, p. 7, 2018.
- [22] G. Wang, H. Laga, J. Jia, N. Xie, and H. Tabia, "Statistical modeling of the 3D geometry and topology of botanical trees," in *Computer Graphics Forum*, vol. 37, no. 5. Wiley Online Library, 2018, pp. 185–198.
- [23] A. Srivastava, E. Klassen, S. H. Joshi, and I. H. Jermyn, "Shape analysis of elastic curves in Euclidean spaces," *IEEE Transactions on Pattern Analysis and Machine Intelligence*, vol. 33, no. 7, pp. 1415–1428, 2011.

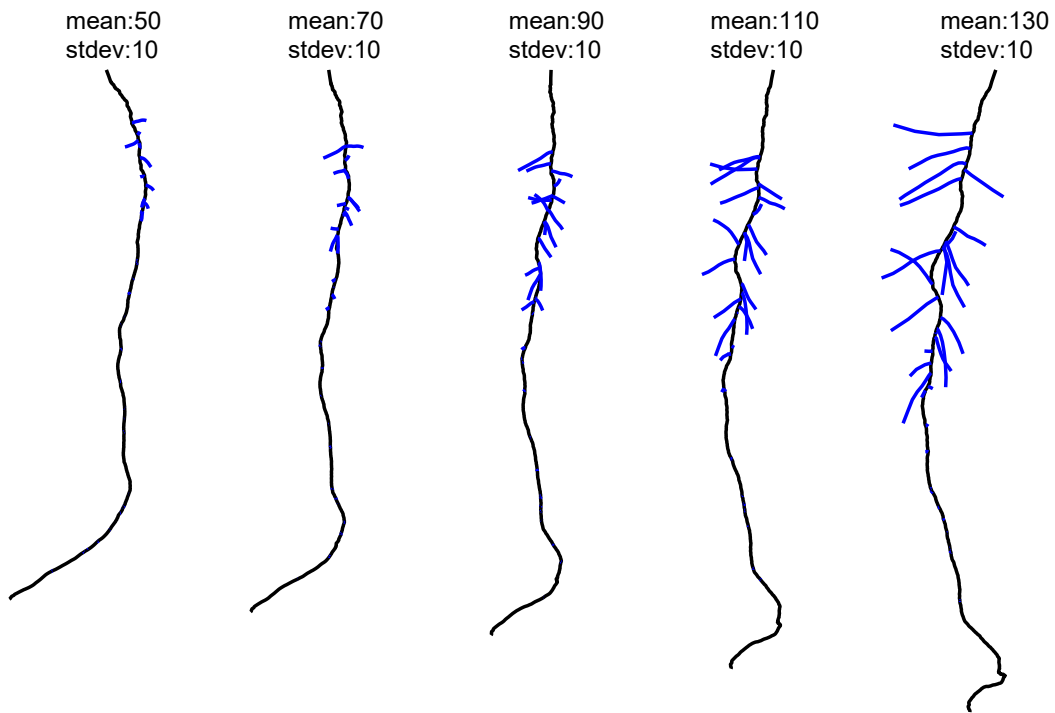


Fig. 10: We consider the mean and standard deviation of the lengths of the lateral branches. The root shapes have been generated by fixing the standard deviation of the length of the lateral roots and varying the value of the mean of the lateral root lengths.

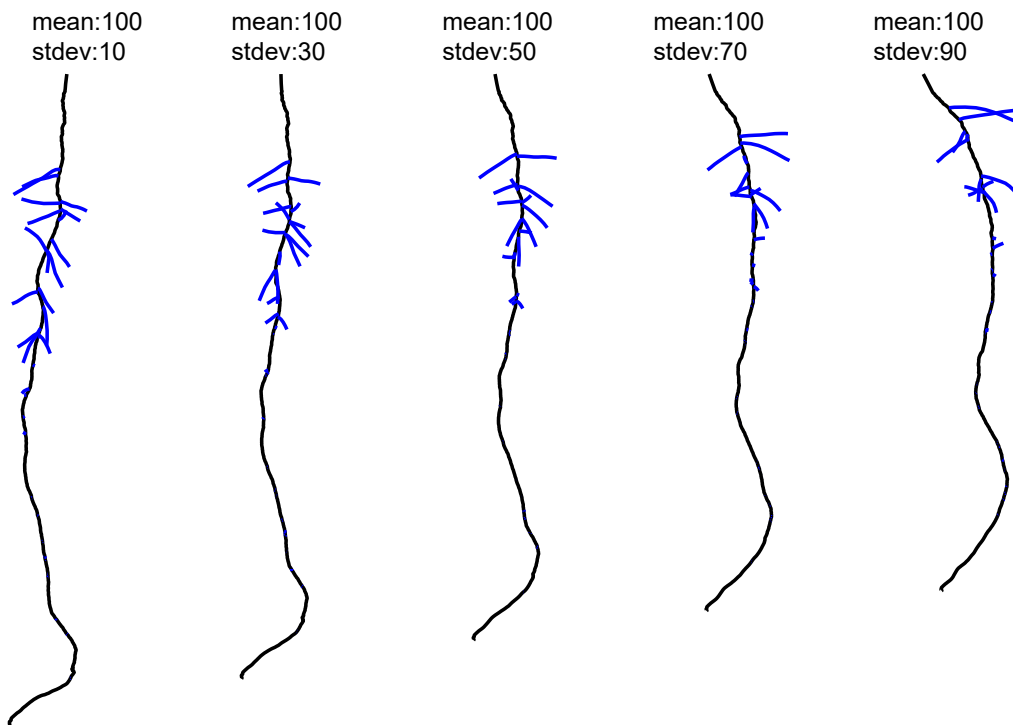


Fig. 11: We consider the mean and standard deviation of the lengths of the lateral roots. The figure shows root shapes generated by fixing the value of the mean of the lateral root lengths and varying the standard deviation of the length of the lateral roots.

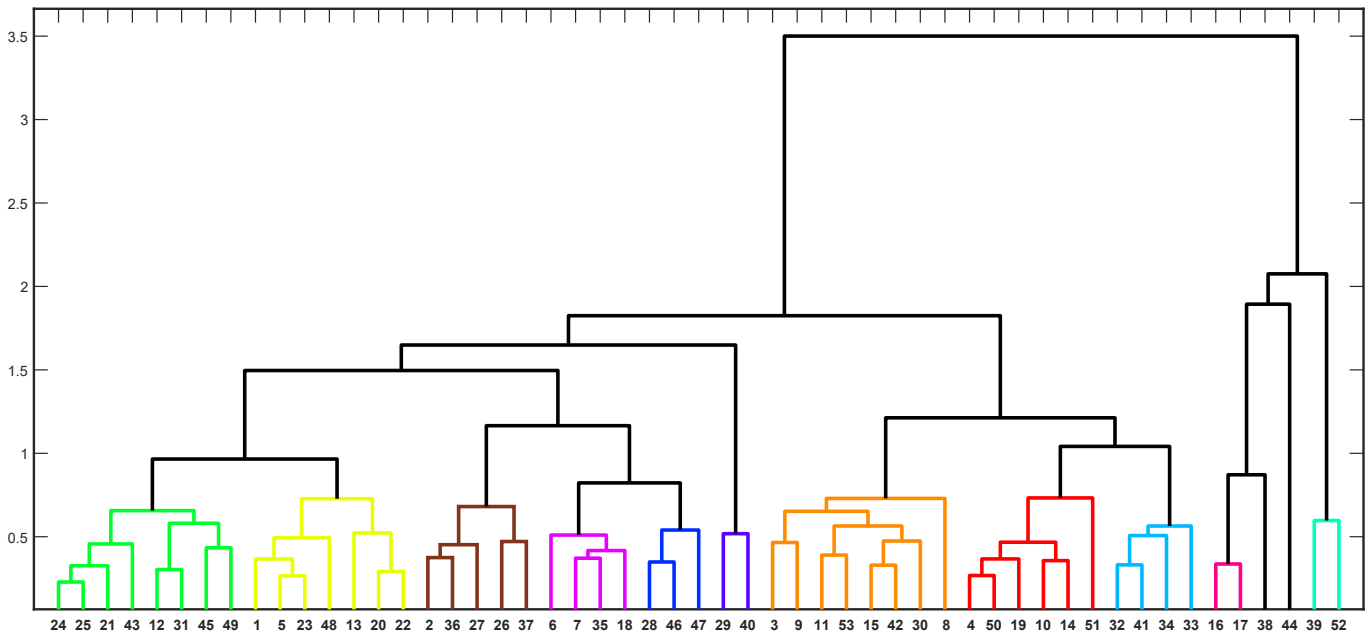


Fig. 12: The hierarchical binary clustering result of the roots in Figure 13.

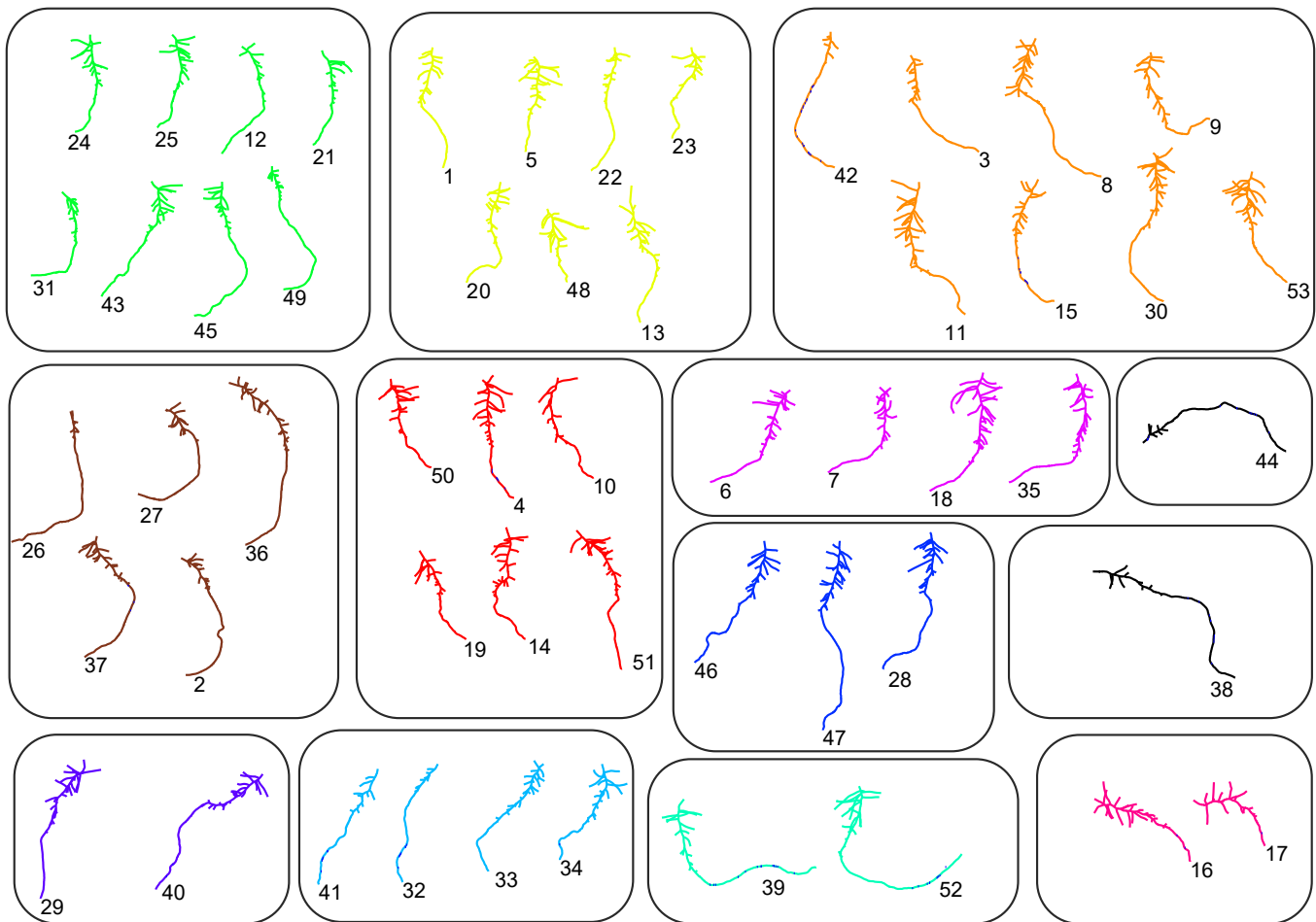


Fig. 13: The clustering results for input roots in accordance with the results of Figure 12. Roots within each cluster are drawn using the same color.